ELSEVIER

Marine and Petroleum Geology 22 (2005) 613–621

Marine and Petroleum Geology

www.elsevier.com/locate/marpetgeo

Seep carbonates and preserved methane oxidizing archaea and sulfate reducing bacteria fossils suggest recent gas venting on the seafloor in the Northeastern South China Sea

Duo Fu Chen[a,b,*], Yong Yang Huang[c], Xun Lai Yuan[d], Lawrence M. Cathles III[e]

[a]*Key Laboratory of Marginal Sea Geology, Guangzhou Institute of Geochemistry and South China Sea Institute of Oceanology, Chinese Academy of Sciences, Wushan, Guangzhou, Guangdong 510640, People's Republic of China*

[b]*Guangzhou Center for Gas Hydrate Research, Chinese Academy of Sciences, Wushan, Guangzhou, Guangdong 510640, China*

[c]*Guangzhou Marine Geological Survey, MGMR, Guangzhou 510075, China*

[d]*Nanjing Institute of Geology and Palaeontology, Chinese Academy of Sciences, 39 East Beijing Road, Nanjing 210008, People's Republic of China*

[e]*Department of Earth and Atmospheric Sciences, Cornell University, Ithaca, NY 14853, USA*

Received 21 September 2004; received in revised form 5 May 2005; accepted 7 May 2005

Abstract

Seep carbonates, formed by the synergistic metabolism of methane oxidizing archaea (MOA) and sulfate reducing bacteria (SRB), have been found in many places worldwide but have not been found to date in the South China Sea. Mud volcanoes and shale diapirs have been reported in the South China Sea however, and microscope and geochemical analysis of carbonates dredged where bottom simulating reflectors (BSR) suggest the presence of gas hydrate on the northeastern continental slope of the South China Sea suggest that the carbonates are hydrocarbon seep-related carbonates. The carbonates we dredged are chimney-like and preserve MOA/SRB fossils. Their very light carbon isotopic compositions (−51.25 to −51.76‰) suggest that their carbon was derived from microbial methane oxidization. These seep carbonates and their preserved MOA/SRB fossils imply gas venting has occurred recently on the seafloor in the northeastern continental slopes in the South China Sea.

Keywords: Seep carbonate; Methane oxidizing archaea; Sulfate reducing bacteria; Gas hydrate; South China Sea

1. Introduction

The marine sediments 1000–7000 m thick (McDonnell et al., 2000) with an organic matter content of 0.46–1.9% (Wu et al., 2003) on the northern continental slope of the South China Sea are a large potential source of natural gas. Water depths are sufficient for gas hydrate to accumulate (Chen et al., 2001, 2004a; Jin and Wang, 2002; McDonnell et al., 2000; Shyu et al., 1998) and geophysical evidence of bottom simulating reflectors (BSR) has been found in reflection seismic records at many locations in the South China Sea (Chow et al., 2000; Chi et al., 1998; Fu et al., 2001; Song et al., 2001; Wu et al., 2005). However, mud volcanoes and shale diapirs are reported only off Taiwan (Chi et al., 1998; Chow et al., 2000, 2001) and in the Qiangdongnan Basin (Chen et al., 2004a) in the South China Sea. To date, seep carbonates have not been found.

Gas and pore water vents are common on continental shelves and slopes worldwide (Aharon, 1994; Dimitrov, 2002; Judd et al., 2002; Kopf, 2003; Mazurenko and Soloviev, 2003; Milkov et al., 2003). Carbonates form at gas seeps as the result of the synergistic oxidization of methane by MOA (methane oxidizing archaea) and the reduction of sulfate by SRB (sulfate reducing bacteria; Valentine and Reeburgh, 2000). The carbonates form mainly during the waning stages of gas venting when the venting rate is slow (Chen et al., 2004b; Roberts and Aharon, 1994; Roberts and Carney, 1997) and have been found throughout the world in ancient sediment as well as at recent gas vents (e.g. Aharon,

* Corresponding author. Address: Key Laboratory of Marginal Sea Geology, Guangzhou Institute of Geochemistry and South China Sea Institute of Oceanology, Chinese Academy of Sciences, Wushan, Guangzhou, Guangdong 510640, People's Republic of China. Tel.: +86 20 85290286; fax: +86 20 8529 0130.

E-mail address: cdf@gig.ac.cn (D.F. Chen).

0264-8172/$ - see front matter © 2005 Elsevier Ltd. All rights reserved.
doi:10.1016/j.marpetgeo.2005.05.002

1994; Cavagna et al., 1999; Peckmann et al., 2001, 2002; Rad et al., 1996; Roberts and Aharon, 1994; Stakes et al., 1999). Deepwater gas vents are also commonly the sites of gas hydrate accumulation (Mazurenko and Soloviev, 2003; Milkov, 2000) where the venting gases are only partially crystallized to hydrate in the subsurface (Cathles and Chen, 2004; Chen et al., 2004b; Chen and Cathles, 2003). Seep carbonates, chemosynthetic communities and gas hydrate accumulation thus are diagnostic of sites of seafloor gas venting (Brooks et al., 1984, 1986; Kennicutt et al., 1988; Mazurenko and Soloviev, 2003; Roberts, 1996, 2001; Roberts and Aharon, 1994; Roberts and Carney, 1997; Sassen et al., 2001).

This paper discusses carbonates collected on the seafloor of the northeastern South China Sea and shows that these carbonates probably formed at gas vents. Active gas venting has direct implication for gas exploration and hydrate accumulation in that area.

2. Sample and analysis

The carbonates described here were collected using a tow-net sampler in April 2002 from the seafloor at 118° 54′E, 22° 07′N in the northeastern continental slope (slope angle ~4°) in the South China Sea. Water depth in the sampled area is ~1000 m. Recently seismic surveys indicate that BSRs are widely distributed on the slope off Taiwan and in the northeastern continental slope in the South China Sea including the area where samples were collected (Fig. 1) (Guangzhou Marine Geological Survey, unpublished data; Guo et al., 2004; Liu et al., 2004). When the samples were spread out on deck, we found several pieces of chimney-like and nodular carbonate rocks. Photographs of some carbonate samples are shown in Fig. 2.

The samples were rinsed with fresh water at the time of collection. In preparation for analysis by scanning electron microscope (SEM) and light microscope, we cleaned the samples again with distilled water. Some of samples were treated with 5% HCl to obtain a pyrite residue for SEM observation. The surfaces of all samples for SEM observation were coated with gold for 30 s using a procedure that does not produce artificial nanobacteria-like features (Folk and Lynch, 1997). The SEM photographs were taken using the LEO-1530VP SEM operating at 10–20 kV with a 5–9 mm working distance. Light microscope photographs were taken using the LEICA-DMRX light microscope.

The samples from the northeastern South China Sea and from a gas seep in Green Canyon 238 in the Gulf of Mexico were crushed to small grains, and thoroughly cleaned in an ultrasonic bath using double distilled de-ionized water. The samples were then milled to less than 200 mesh powder. The wt% of minerals was determined by the peak amplitude method of X-ray diffraction (XRD) (Table 1). Calcite and

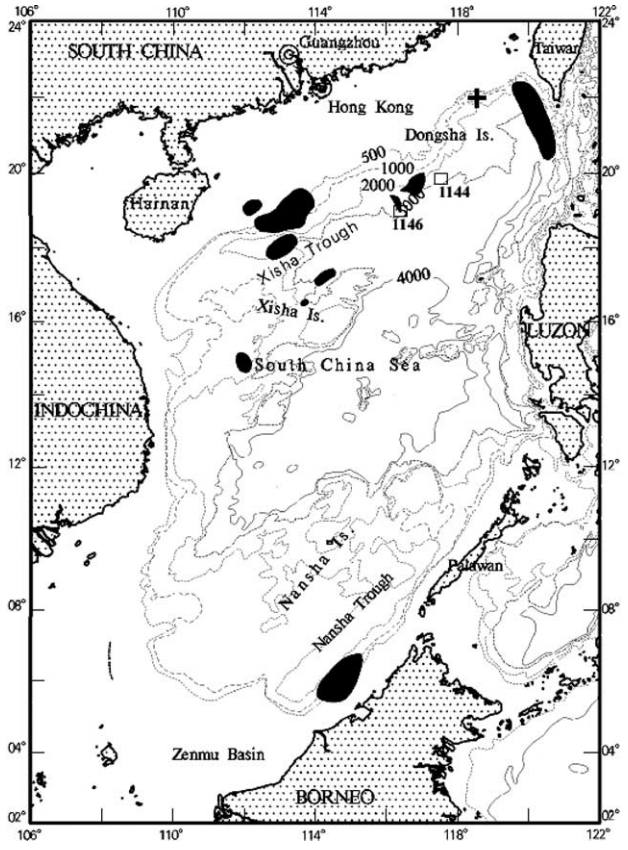

Fig. 1. Bathymetry and BSR distributions for possible gas hydrate occurrence in the South China Sea (Guo et al., 2004). Black areas indicate the distribution of some BSRs in the South China Sea. More recently seismic data indicate that BSRs (not shown here) are widely distributed on the slope off Taiwan and on the northeastern continental slope in the South China Sea including the area where samples were collected (Guangzhou Marine Geological Survey, unpublished data; Liu et al., 2004). The numbers 1144 and 1146 with squares indicate the location of ODP Leg 184 Sites. The cross is the location where we collected samples.

pyrite were determined by using the Oxford-INCA300 EDS capability of the SEM, light microscope, and XRD.

Carbon and oxygen isotopic ratios were measured by a Finnigan MAT 252 mass spectrometer. Replicate analyses of a laboratory standard yielded standard deviations less than 0.01% for both $\delta^{18}O$ and $\delta^{13}C$ values. All carbon and oxygen isotopic data for the carbonates reported here are in permil (‰) relative to PeeDee Belemnite (PDB) standard.

Half gram of sample powder was treated with 50 ml of 5% HNO_3 in a pre-weighed centrifuge tube for 2–3 h to separate the carbonate mineral phase and residue phase, then 2500 ng of Rhodium was added as an internal standard for calculating the concentration of the rare earth elements (REE) in the 5% HNO_3 dissolved-solution of carbonate mineral phase. The samples were then centrifuged to separate a residue from the 5% HNO_3 dissolved-solution (carbonate minerals). Five milliliters of this solution was diluted 10 times for the analysis of the REE. The residue and the tube were weighed and the percentage of residue and carbonate mineral calculated (Table 1). Five to ten

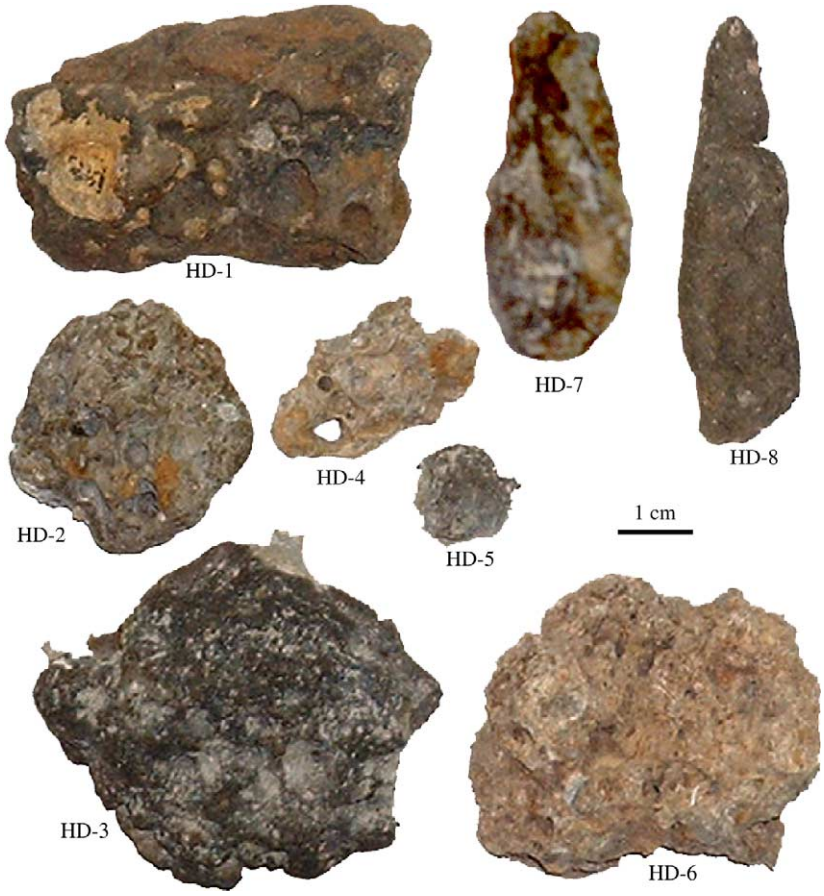

Fig. 2. Photographs of some of the carbonate crusts collected on the seafloor in the northeastern South China Sea. HD-7 and HD-8 are the chimney-like carbonates, and others are the nodular carbonate samples.

milligrams of residue was used for REE analysis. The chemical procedure for the REE analysis of the residue was described in Chen et al. (2003). Precision and accuracy was checked by the analyses of two proficiency-testing samples, GBPG-1 and OU-6. The average relative standard deviations are better than 5% for the REE. The whole rock composition agrees well with that which we calculate by combining our analysis of the soluble and insoluble parts of the carbonate samples (Tables 1 and 3).

3. Results

3.1. Chimney-like carbonate

The chimney-like carbonates we dredged from the seafloor in the northeastern continental slopes in the South China Sea are semi-solidified, ~4–6 cm long, ~0.5–1 cm in diameter on their small end, and ~1–2 cm in diameter on their large end (Fig. 2). Our X-ray analysis shows that

Table 1
Mineral composition in the carbonates determined by X-ray diffraction (%)

Minerals	HD-6	HD-3	HD-7	S-4-1	S-4-2
	Brecciated carbonate	Coralline carbonate	Chimney-like carbonate	Seep carbonate from GC 238, Gulf of Mexico	
Chlorite	8.1	–	–	–	–
Illite	12.2	–	12.2	7.2	6.1
Quartz	10.2	7.2	6.2	3.1	2.2
Plagioclase	8.3	4.8	–	–	–
Calcite	60.1	82.2	76.1	89.1	91.1
Aragonite	–	6.1	–	–	–
Unknown	–	–	5.1	–	–
Total	98.9	100.3	99.6	99.4	99.4
Soluble phase	N	86.7	58.0		84.4
Residual phase	N	13.3	42.0		15.6

Soluble phase and residual phase is the 5% HCl-dissolved mineral phase and residual mineral phase, respectively. N is not analyzed.

the chimney-like carbonates mainly consist of calcite, illite, quartz, and an unknown mineral, and are identical mineralogically to seep carbonates we have sampled from gas vents in the Gulf of Mexico (Table 1). Transmitted light microscope observation of the interior of these samples shows microbial filaments (Fig. 3a and b). The diameter of these microbial filament ranges from 0.08 to 0.46 μm but are mainly 0.2–0.4 μm (Fig. 4a). The SEM images show small microbial spheroids ($<\sim$0.3 μm in diameter) on interior surfaces and a microbial layer ($\sim$0.5 μm thick) on the outer surface of the sample (Fig. 3c). Reflected light microscopy shows that pyrite occurs as spheroidal and irregular aggregates, and as chains and filaments (Fig. 3d). The spheroidal and irregular aggregates consist of numerous smaller spheroids and rods (Fig. 3d1-3 and d6-10) with calcite in the center of the aggregates (Fig. 3d6-7). The chains and filaments form by the connection of individual rods (Fig. 3d4-5). Thin section measurement using the LEICA-DMRX optical microscope with the Leica Qwin Program shows that the size of pyrite aggregate ranges from

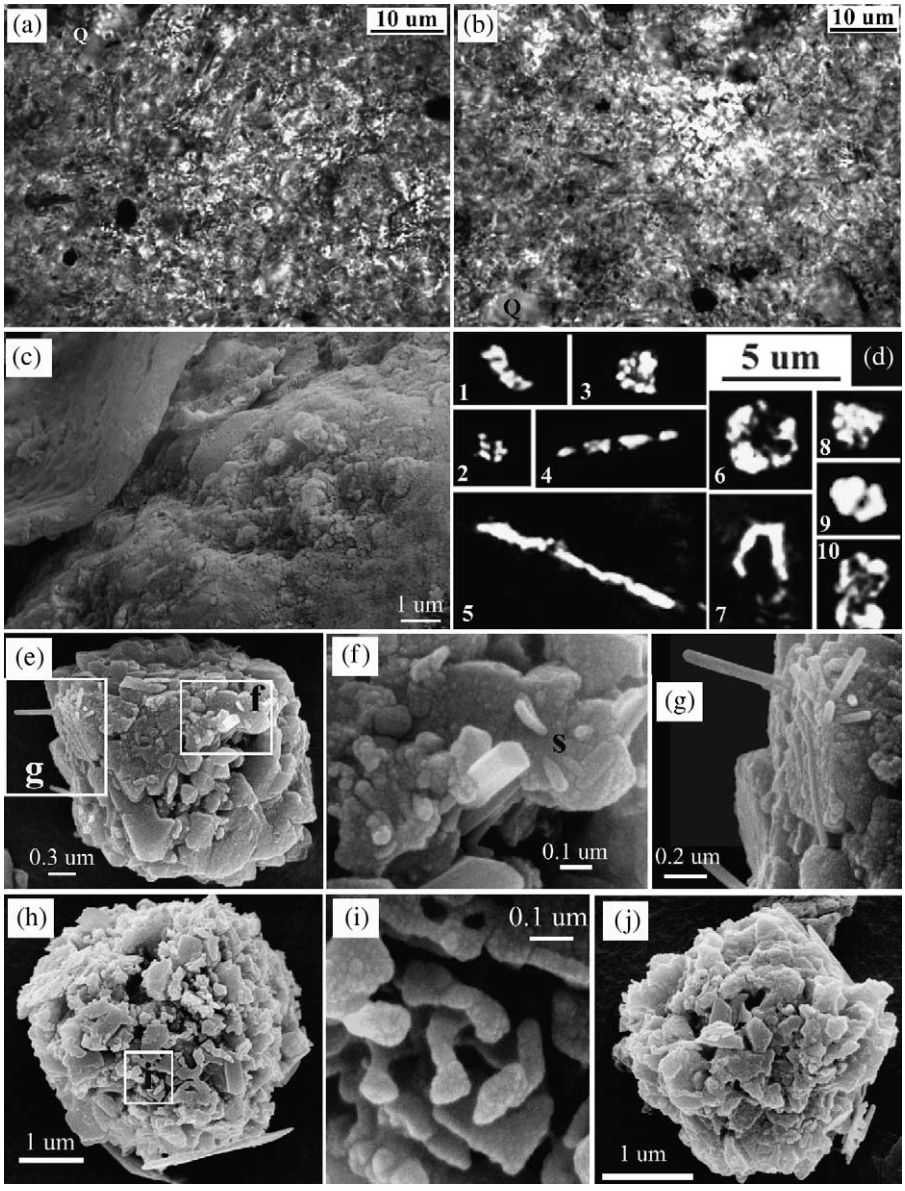

Fig. 3. The microscope images of the chimney-like carbonates. (a) and (b) are transmitted light microscope images of the chimney-like carbonates. The chimney-like carbonate consists of calcites, pyrite (deep black colure), clay and quartz (marked by Q), and microbial filaments. (c) is the SEM image of the freshly fractured surface of the chimney-like carbonate. The interior shows small microbial spheroids $<\sim$0.3 μm in diameter. A microbial layer $\sim$0.5 μm thick is present on the outer surface of the sample. (d) is the reflected light microscope image of the pyrite spheroids, chains, and filaments. The chains and filaments consist of small rods $<$0.3 μm in diameter. The spheroidal and irregular aggregates are composed of numerous smaller spheroids and rods 0.2–1.5 μm in diameter that surround a calcite core. (e)–(i) are SEM images of pyrite spheroids in the 5% HCl treated-residues. The pyrite spheroids consist of non-crystalline and crystalline pyrite. (f) and (g) are enlargements of the white area in (e), and f shows the nanomicrobial ovoids (marked 'S') dispersed on the surface. (i) is enlargement of the white area in h showing chains of nanomicrobial filaments $<$0.1 μm in diameter.

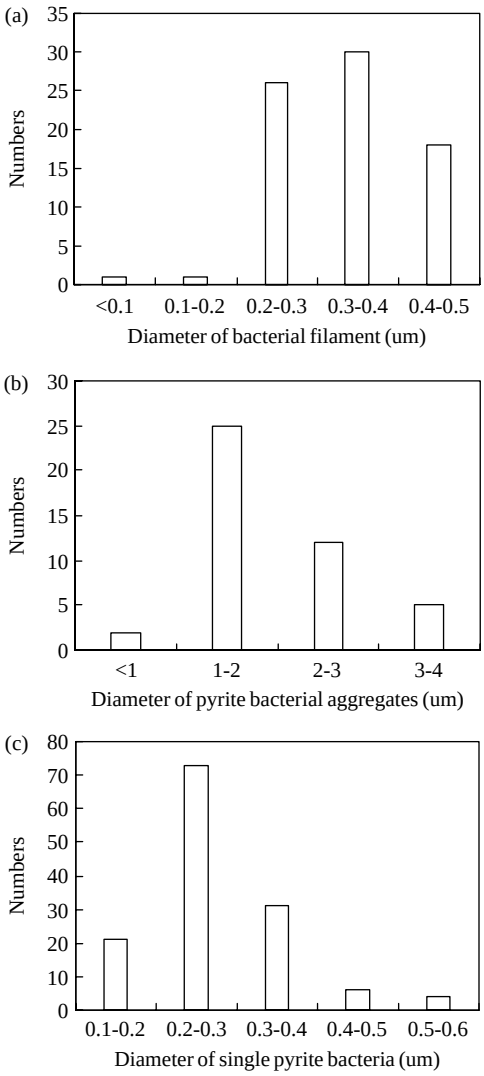

Fig. 4. The statistical distribution of the diameters of microbial aggregate filaments (a), pyrite microbial aggregates (b), and single bacteria (c), measured from thin sections using the Leica-DMRX microscope with the Leica Qwin Program.

0.8 to 3.7 μm in diameter with a mean value of 1.9 μm (Fig. 4b). The smaller spheroids and rods are 0.13–0.48 μm in diameter with a mean value of 0.28 μm (Fig. 4c). Our SEM images show that the pyrite spheroidal aggregate is composed of non-crystalline and crystalline pyrite (Fig. 3e–j). The nanomicrobial ovoides (labeled 'S') are <0.1 μm in diameter and are dispersed on the surface (Fig. 3f). The rods connect together to form filaments (Fig. 3i).

The $\delta^{13}C_{PDB}$ and $\delta^{18}O_{PDB}$ of the carbonate minerals of the chimney-like carbonates is very uniform from -51.25 to $-51.76‰$ and from 4.76 to 5.11‰, respectively (Table 2). The shale-normalized REE patterns of the 5% HNO_3-treated solution (carbonate minerals) show no Ce and Eu anomalies, slight LREE depletion and slight MREE enrichment. The REE patterns of the 5% HNO_3-treated residue show the flat REE pattern that is typical of shale (Table 3 and Fig. 5).

Table 2
The oxygen and carbon isotopic compositions of carbonates

Sample	Name	$\delta^{13}C_{PDB}‰$	$\delta^{18}O_{PDB}‰$
Northeastern South China Sea			
HD-7-1	Chimney-like carbonate	−51.76	5.02
HD-7-2	Chimney-like carbonate	−51.59	5.11
HD-8	Chimney-like carbonate	−51.25	4.76
HD-3	Coralline carbonate	0.38	0.62
HD-6	Brecciated carbonate	0.28	0.37
Green Canyon 238 in the Gulf of Mexico			
S-4-1	Seep carbonate	−52.22	4.53
S-4-2	Seep carbonate	−52.29	4.35
S-4-3	Seep carbonate	−51.95	4.06

3.2. Nodular carbonates

In addition to chimney-like seep carbonates, there are also nodular carbonates including brecciated carbonates and coralline carbonates. Brecciated carbonates consist of rounded carbonate pebbles of calcite that are cemented together with calcite. The calcite crystals in the cement are larger in size than crystals in the pebbles. The X-ray analysis shows that the brecciated carbonates consist of calcite, clay minerals, quartz, and plagioclase, while the coralline carbonates consist of calcite, aragonite, quartz, and plagioclase (Table 1). The microscope observation of coralline carbonates shows that carbonates contain mainly the crustose coralline algaes of *Lithothamnium*, and *Mesophyllum* with some attached cyclostomate bryozoans, as well as the debris of hexacorals and gastropods. These two genera both have thicker perithallium. The hypothallium of *Lithothamnium* is mutilayered simple form, while the hypothallium of *Mesophyllum* is mutilayered coaxial forms. These organisms usually live in shallow shelf environments where the water depth is <250 m (Wray, 1977).

The $\delta^{13}C_{PDB}$ of the carbonate minerals of the brecciated carbonate and the coralline carbonate is 0.28 and 0.38‰, respectively, while $\delta^{18}O_{PDB}$ is 0.37 and 0.62‰, respectively (Table 2). These isotopic values are typical of the marine carbonate. The shale-normalized REE pattern of the 5% HNO_3-treated solution derived from the carbonate minerals of the coralline carbonate shows a negative Ce anomaly, and slight LREE depletion and slight MREE enrichment. However, the REE pattern of the 5% HNO_3-treated residue (illite and quartz) again shows the typical flat REE pattern of shale (Table 3 and Fig. 5). These carbonates have a different REE pattern and isotopic ratio than the chimney-like carbonates. We believe that these nodular carbonates may have been possible transported down the $\sim4°$ slope to the dredge site from a more northern location where the water depth was <250 m.

Table 3
The REE contents in whole rocks, soluble and insoluble parts of carbonate samples

Elements	GBPG-1		OU-6		HD-7				HD-3				S-4			
	Ref	Anal	Ref	Anal	Resi	Solu	WR	CA	Resi	Solu	WR	CA	Resi	Solu	WR	CA
La	52.95	52.53	33.00	35.84	26.97	11.29	17.81	17.87	29.87	3.66	7.81	7.15	21.29	2.87	6.14	5.74
Ce	103.20	97.93	74.42	75.31	51.28	21.77	34.06	34.16	54.44	5.66	14.27	12.15	37.12	6.23	11.56	11.05
Pr	11.45	11.61	7.80	8.49	5.94	2.57	3.94	3.98	6.58	0.94	1.82	1.69	4.27	0.75	1.34	1.30
Nd	43.30	41.93	29.01	30.84	20.23	10.44	14.25	14.55	22.13	4.03	7.04	6.44	13.88	2.91	4.71	4.63
Sm	6.79	6.59	5.92	5.87	3.50	2.53	2.80	2.94	3.91	1.00	1.47	1.39	2.11	0.64	0.94	0.87
Eu	1.79	1.76	1.36	1.33	0.62	0.58	0.62	0.60	0.72	0.26	0.35	0.32	0.43	0.14	0.21	0.18
Gd	4.74	4.91	5.27	5.23	2.73	2.75	2.71	2.74	3.15	1.11	1.42	1.38	1.81	0.58	0.83	0.77
Tb	0.60	0.62	0.85	0.84	0.45	0.42	0.43	0.43	0.47	0.17	0.23	0.21	0.29	0.09	0.13	0.12
Dy	3.26	3.33	4.99	5.18	2.79	2.47	2.51	2.61	3.04	0.99	1.25	1.27	1.75	0.49	0.65	0.69
Ho	0.69	0.71	1.01	1.07	0.57	0.51	0.54	0.53	0.61	0.19	0.25	0.25	0.37	0.10	0.14	0.14
Er	2.01	2.22	2.98	3.17	1.78	1.43	1.61	1.58	1.95	0.54	0.70	0.72	1.25	0.26	0.43	0.41
Tm	0.30	0.33	0.44	0.46	0.26	0.20	0.23	0.23	0.30	0.07	0.10	0.10	0.20	0.04	0.06	0.06
Yb	2.03	2.25	3.00	3.22	1.81	1.24	1.43	1.48	1.92	0.42	0.60	0.62	1.33	0.19	0.39	0.37
Lu	0.31	0.34	0.45	0.45	0.28	0.20	0.23	0.24	0.29	0.06	0.08	0.09	0.21	0.03	0.06	0.06
ΣREE					119.22	58.39	83.18	83.94	129.39	19.11	37.39	33.78	86.28	15.32	27.58	26.39
Ce/Ce*					0.96	0.91	0.95	0.94	0.93	0.69	0.87	0.81	0.92	1.00	0.95	0.95
Eu/Eu*					0.95	1.03	1.06	0.99	0.97	1.15	1.15	1.09	1.04	1.05	1.11	1.05

Ref and Anal are the reference data and analytical data of the standard reference, respectively. Resi and Solu are the 5% HCl dissolved-residues and solution, respectively. WR is the analyzed data of whole rock of carbonate samples. CA is the calculated value from a re-combination of our analysis of soluble and insoluble parts and the contents of soluble and insoluble parts of the samples listed in Table 1. The Ce/Ce* denotes $3Ce_N/(2La_N+Nd_N)$, Eu/Eu* denotes $Eu_N/(Sm_N+Gd_N)^{0.5}$, where $_N$ refers to normalization of concentrations against the standard Post Archean Australian Shale (McLennan, 1989).

4. Discussion

The filaments, spheroids, rods, and ovoids observed in the chimney-like carbonates collected from the seafloor in the northeastern South China Sea are identical to those found in the seep carbonates in a gas vent in Green Canyon 238 in the Gulf of Mexico (Chen et al., unpublished data). The rod-chain structure is identical to that of MOA/SRB observed in methane-seep sediments from Eel River Basin (Orphan et al., 2002). The pyrite spheroid shows a layer structure in which a calcite center is surrounded by a shell of pyritic microbial fossils. These rod-chain and layer structure fossils display the collaborating form that is characteristic of living MOA/SRB colonies (Boetius et al., 2000; Orphan et al., 2001, 2002). The collaborating form has also been found in the seep carbonates from Green Canyon 238 in the Gulf of Mexico (Chen et al., unpublished data).

The nanometer scale (0.3–0.025 μm) of some of the spheroids, rods and ovoids in the South China Sea samples classifies them as nanobacteria according to Folk and his colleagues (Folk, 1993, 1999; Folk and Lynch, 2001; Folk and Rasbury, 2002). These nanobacteria may be MOA and SRB in an early stage of development.

Carbon isotopic ratios of −51.25 to −51.76‰ in the chimney-like carbonates suggest that they are seep carbonate (Aharon, 1994; Cavagna et al., 1999; Peckmann et al., 2001, 2002; Rad et al., 1996; Roberts and Aharon, 1994; Stakes et al., 1999) that was initially precipitated at a site of gas venting where MOA/SRB collaborated to oxidize the venting methane to CO_2 while also reducing seawater sulfate to H_2S (Valentine and Reeburgh, 2000). The carbon isotopic ratios and REE patterns in the chimney-like carbonates in the northeastern South China Sea are identical to those found in seep carbonates from a gas vent site in Green Canyon 238 in the Gulf of Mexico, but are very different from those of nodular carbonates collected with the chimney-like carbonates.

Calcite precipitated in equilibrium with bottom water ($\delta^{18}O$ water $\approx 0‰ \pm 0.2‰$; SMOW) at 3–4 °C (the temperature at ~1000 m water depth in the South China Sea where the samples reported here were collected; Xue et al., 1991) has a $\delta^{18}O_{PDB}$ value of approximately 3.23–3.50‰, according to Epstein et al. (1953). The chimney-like carbonates in the northeastern South China Sea show a $\delta^{18}O_{PDB}$ values of 4.76–5.11‰. An explanation for a $\delta^{18}O$ enrichment is therefore needed. A $\delta^{18}O$ enrichment of seep carbonates has been observed in a number of gas vent sites (Aloisi et al., 2000; Bohrmann et al., 1998; Matsumoto, 1990; Stakes et al., 1999). Gas hydrate preferentially incorporates water enriched in ^{18}O (Davidson et al., 1983; Sloan, 1998). When gas hydrates decompose, water significantly enriched in ^{18}O is produced. This isotopically heavy water could be incorporated in the carbonates, explaining their observed oxygen isotopic enrichment (Aloisi et al., 2000; Bohrmann et al., 1998; Matsumoto, 1990; Stakes et al., 1999). However, there is also an alternative mechanism of $\delta^{18}O$ enrichment of seep carbonates at gas vent sites. Detailed studies of some sites (e.g. at the Hydrate Ridge offshore Oregon, Suess et al., 1999) indicate that no significant hydrates decompose at the base of the gas hydrate stability zone, and the majority of the gas at vent sites at the Hydrate Ridge possibly derives from the deeply buried petroleum systems (Milkov et al., 2005), suggesting that pore water for carbonate precipitation near

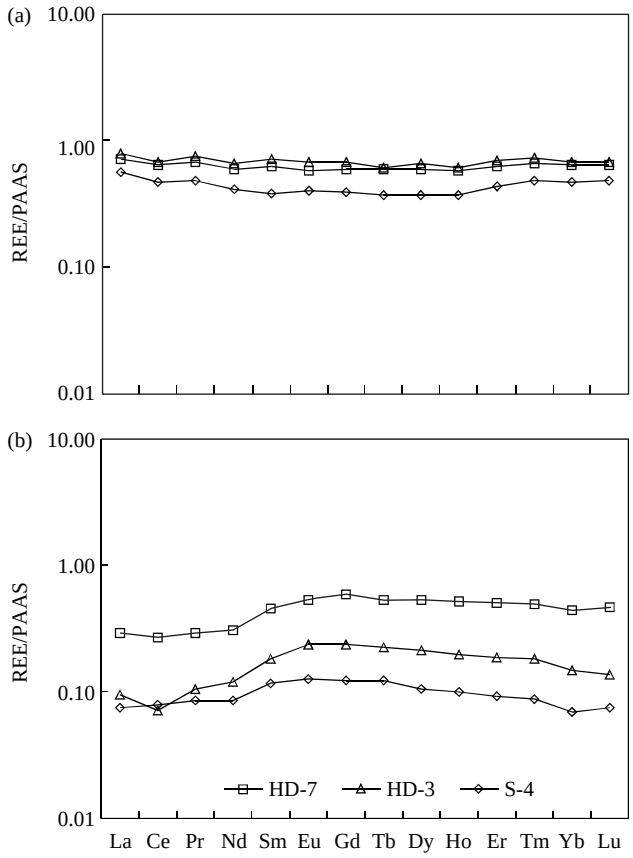

Fig. 5. Shale-normalized REE patterns of carbonate. (a) and (b) is the 5% HCl treated-residue and solution, respectively. HD-3 is the nodular coralline carbonate, HD-7 is the chimney-like carbonate, and S-4 is the seep carbonate in Green Canyon 238 in the Gulf of Mexico.

the seafloor also has a deep source. The smectite–illite transition generates pore water that is depleted in Cl^- and enriched in ^{18}O, and the advection of such pore water along migration pathways to seafloor vent sites would provide a source of ^{18}O-enriched pore water for carbonate precipitation (e.g. Hesse, 2003).

5. Conclusions

The chimney-like carbonates collected in the northeastern South China Sea preserve the spheroids, rods, ovoids and filaments of microbial microfossils. A shell of aggregated bacteria surrounds central microbial aggregates and microbial rods form chains suggesting the fossils are collaborating colonies of methane oxidizing archaea and sulfate reducing bacteria (MOA/SRB). The carbon isotopic composition of the chimney-like carbonates indicates that their carbon was sourced from microbial methane oxidization. These characteristics suggest the chimney carbonates formed where gas vented from the seafloor in the South China Sea. The chimney carbonates could have been transported, as we believe the nodular carbonates were transported, and the site of origin is thus uncertain. The vents, however, must have been deep enough for hydrate crystallization, if our interpretation is correct. Deep gas venting in the South China Sea may have important implication for gas exploration and gas hydrate accumulation.

Acknowledgements

This study was partially supported by the Chinese Academy of Sciences (Projects: KZCX3-SW-224 and KGCX2-SW-309), the NSFC (Grant: 40472059), and Guangzhou Institute of Geochemistry of Chinese Academy of Sciences (GIGCX-03-04; GIGCX-04-03). Funds from the corporate sponsors of the Global Basins Research Network supported Chen in the U.S. Chen D. F. and Cathles L. M. are grateful to Roberts H. H. and the Minerals Management Service for encouragement of the work, especially for an invitation to participate on a submersible investigation of Gulf of Mexico during which the seep carbonates were collected in Green Canyon 238. Chen D. F. also is indebted the help from Chen Guangqian for sample collection on board from the South China Sea and Qi Liang for REE analysis. Finally we are pleased to acknowledge helpful comments from reviewers H. Roberts, A. V. Milkov, and editor D. G. Roberts.

References

Aharon, P., 1994. Geology and biology of modern and ancient submarine hydrocarbon seeps and vents: an introduction. Geo-marine Letters 14, 69–73.

Aloisi, G., Pierre, K., Rouchy, J., Forney, L.J., Woodside, J., The MEDINAUT Scientific Party, 2000. Methane-related authigenic carbonates of eastern Mediterranean Sea mud volcanoes and their possible relation to gas hydrate destabilization. Earth and Planetary Science Letters 184, 321–338.

Boetius, A., Ravenschlag, K., Schubert, C.J., Rickert, D., Widdel, F., Gieseke, A., et al., 2000. Amarinemicrobial consortium apparently mediating anaerobic oxidation of methane. Nature 407, 623–626.

Bohrmann, G., Greinet, J., Suess, E., Torres, M., 1998. Authigenic carbonates from the Cascadia subduction zone and their relation to gas hydrate stability. Geology 26, 647–650.

Brooks, J.M., Kennicutt II., M.C., Fay, R.R., McDonald, T.J., Sassen, R., 1984. Thermogenic gas hydrates in the Gulf of Mexico. Science 225, 409–411.

Brooks, J.M., Cox, H.B., Bryant, W.R., Kennicutt II., M.C., Mann, R.G., McDonald, T.J., 1986. Association of gas hydrates and oil seepage in the Gulf of Mexico. Organic Geochemistry 10, 221–234.

Cathles, L.M., Chen, D.F., 2004. A compositional kinetic model of hydrate crystallization and dissolution. Journal of Geophysics Research, 109, B08102, doi:10.1029/2003JB002910.

Cavagna, S., Clari, P., Martire, L., 1999. The role of bacteria in the formation of cold seep carbonates. Geological evidence from Monferrato (Tertiary, NW Italy). Sedimentary Geology 126, 253–270.

Chen, D.F., Cathles, L.M., 2003. A kinetic model for the pattern and amounts of hydrate precipitated from a gas steam: application to the Bush Hill vent site Green Canyon Block 185, Gulf of Mexico. Journal Geophysics Research 108, 2058. doi:10.1029/2001JB001597.

Chen, D.F., Zhao, Z.H., Yao, B.C., 2001. Predicted pressure–temperature and thickness below seafloor of gas hydrate formation of natural gases from Ya-13 gas field in Qiangdongnan basin in the northern margin of South China Sea. Geochemica 30, 585–591 (in Chinese).

Chen, D.F., Dong, W.Q., Qi, L., Chen, G.Q., Chen, X.P., 2003. Possible REE constrains on the depositional and diagenetic environment of Doushantuo formation phosphorites containing the earliest metazoan fauna. Chemical Geology 201, 103–118.

Chen, D.F., Cathles, L.M., Roberts, H.H., 2004a. The chemical signatures of variable gas venting at hydrate sites. Marine and Petroleum Geology 21 (3), 317–326.

Chen, D.F., Li, X.X., Xia, B., 2004b. Distribution of gas hydrate stable zone and resource prediction in Qiongdongnan basin in South China Sea. Chinese Journal of Geophysics 47 (3), 483–489 (in Chinese).

Chi, W.C., Reed, D.L., Liu, C.S., Lundberg, N., 1998. Distribution of the bottom-simulating reflector in the offshore Taiwan collision zone. Terrestrial Atmospheric and Oceanic Sciences 9, 779–794.

Chow, J., Lee, J.S., Sun, R., Liu, C.S., Lundberg, N., 2000. Characteristics of the bottom simulating reflectors near mud diapirs: offshore southwestern Taiwan. Geo-Marine Letters 20, 3–9.

Chow, J., Lee, J.S., Liu, C.S., Lee, B.D., Watkins, J.S., 2001. A submarine canyon as the cause of a mud volcano—Liuchieuyu Island in Taiwan. Marine Geology 176, 55–63.

Davidson, D.W., Leaist, D.J., Hesse, R., 1983. Oxygen-18 enrichment in water of a clathrate hydrate. Geochimica et Cosmochimica Acta 47, 2293–2295.

Dimitrov, L.I., 2002. Mud volcanoes—the most important pathway for degassing deeply buried sediments. Earth-Science Reviews 59, 49–76.

Epstein, S., Buchsbaum, R., Lowenstam, H., Urey, H.C., 1953. Revised carbonate–water isotopic temperature scale. Geological Society of America Bulletin 64, 1315–1326.

Folk, R.L., 1993. SEM imaging of bacteria and nannobacteria in carbonate sediments and rocks. Journal of Sedimentary Research 63, 990–999.

Folk, R.L., 1999. Nannobacteria and the precipitation of carbonate in unusual environments. Sedimentary Geology 126, 47–55.

Folk, R.L., Lynch, F.L., 1997. The possible role of nannobacteria (dwarf bacteria) in clay mineral diagenesis and the importance of careful sample preparation in high magnification SEM study. Journal of Sedimentary Research 7, 597–603.

Folk, R.L., Lynch, F.L., 2001. Organic matter, putative nannobacteria and the formation of ooids and hardgrounds. Sedimentology 48, 215–229.

Folk, R.L., Rasbury, E.T., 2002. Nanometre-scale spheroids on sands, Vulcano, Sicily. Possible nannobacterial alteration. Terra Nova 14, 469–475.

Fu, X., Yang, M.Z., Wen, P.F., Xu, H.N., 2001. Seismic data processing and characteristics for gas hydrates in South China Sea. Geological Science and Technology Information 20, 33–40 (in Chinese).

Guo, T.M., Wu, B.H., Zhu, Y.H., Fan, S.S., Chen, G.J., 2004. A review on the gas hydrate research in China. Journal of Petroleum Science and Engineering 41, 11–20.

Hesse, R., 2003. Pore water anomalies of submarine gas-hydrate zone as tool to assess hydrate aboundance and distribution in subsurface: what have we learned in the past decade? Earth-Science Reviews 61, 149–179.

Jin, C.S., Wang, J.Y., 2002. Preliminary study on the gas hydrates stability zone in the South China Sea. Acta Geologica Sinica 76, 423–428 (English edition).

Judd, A.G., Hovland, M., Dimitrov, L.I., Garcia Gil, S., Jukes, V., 2002. The geological methane budget at continental margins and its influence on climate change. Geofluids 2, 109–126.

Kennicutt II., M.C., Brooks, J.M., Denoux, G.J., 1988. Leakage of deep, reservoired petroleum to the near surface of the Gulf of Mexico continental slope. Marine Chemistry 24, 39–59.

Kopf, A.J., 2003. Global methane emission through mud volcanoes and its past and present impact on the Earth's climate. International Journal of Earth Sciences 92, 806–816.

Liu, C., Schurle, P., Chang, H., Chen, K., Chung, S., Wang, Y., Hsiuan, T., 2004. Distribution and Seismic Characteristics of Gas Hydrate Offshore Southwestern Taiwan. Eos. Trans, AGU, 85 (28) (West. Pac. Geophys, Meet. Suppl., Abstract OS23A-04).

Matsumoto, R., 1990. Vuggy carbonate crust formed by hydrocarbon seepage on the continental shelf of Baffin Island, northeast Canada. Geochemical Journal 24, 143–158.

Mazurenko, L.L., Soloviev, V.A., 2003. Worldwide distribution of deep-water fluid venting and potential occurrences of gas hydrate accumulations. Geo-Marine Letter 23, 162–176.

McDonnell, S.L., Max, M.D., Cherkis, N.Z., Czarnecki, M.F., 2000. Tectono-sedimentary controls on the likelihood of gas hydrate occurrence near Taiwan. Marine and Petroleum Geology 17, 929–936.

McLennan, S.M., 1989. Rare earth elements in sedimentary rocks: influence of provenance and sedimentary processes. In: Lipin, B.R., McKay, G.A. (Eds.), Geochemistry and Mineralogy of Rare Earth Elements Min. Soc. Am. Rev. Mineral, vol. 21, pp. 169–200.

Milkov, A.V., 2000. Worldwide distribution of submarine mud volcanoes and associated gas hydrates. Marine Geology 167, 29–42.

Milkov, A.V., Sassen, R., Apanasovich, T.V., Dadashev, F.G., 2003. Global gas flux from mud volcanoes: a significant source of fossil methane in the atmosphere and the ocean. Geophysics Research Letter 30, 4. doi:10.1029/2002GL016358.

Milkov, A.V., Claypool, G.E., Lee, Y.-J., Sassen, R., 2005. Gas hydrate systems at Hydrate Ridge offshore Oregon inferred from molecular and isotopic properties of hydrate-bound and void gases. Geochimica et Cosmochimica Acta 69, 1007–1026.

Orphan, V.J., House, C.H., Hinrichs, K.U., McKeegan, K.D., DeLong, E.F., 2001. Methane-consuming archaea revealed by directly coupled isotopic and phylogenetic analysis. Science 293, 484–487.

Orphan, V.J., House, C.H., Hinrichs, K.U., McKeegan, K.D., DeLong, E.F., 2002. Multiple archaeal groups mediate methane oxidation in anoxic cold seep sediments. Proceedings of the National Academy of Sciences of the United States of America 99, 7663–7668.

Peckmann, J., Reimer, A., Luth, U., Hansen, B.T., Heinicke, C., Hoefs, J., et al., 2001. Methane-derived carbonates and authigenic pyrite from the northwestern Black Sea. Marine Geology 177, 129–150.

Peckmann, J., Goedert, J.L., Thiel, V., Michaelis, W., Reitner, J., 2002. A comprehensive approach to the study of methane-seep deposits from the Lincoln Creek Formation, western Washington State, USA. Sedimentology 49, 855–873.

Rad, U.V., Rosch, H., Berner, U., Geyh, M., Marching, V., Schulz, H., 1996. Authigenic carbonates derived from oxidized methane vented from the Makran accretionary prism of Pakistan. Marine Geology 136, 55–77.

Roberts, H.H., 1996. Surficial geology of the middle and upper continental slope, northern Gulf of Mexico; the important role of episodic fluid venting. AAPG Bulletin 80 (9), 1511.

Roberts, H.H., 2001. Fluid and gas expulsion on the Northern Gulf of Mexico continental slope. Mud-prone to mineral-prone responses. In: Paull, C.K., Dillon, W.P. (Eds.), Natural Gas Hydrates: Occurrence, Distribution, and Detection. American Geophysical Union, Washington, DC, pp. 145–161.

Roberts, H.H., Aharon, P., 1994. Hydrocarbon-derived carbonate buildups of the northern Gulf of Mexico continental slope. a review of submersible investigations. Geo-Marine Letter 14, 135–148.

Roberts, H.H., Carney, R.S., 1997. Evidence of episodic fluid, gas, and sediment venting on the northern Gulf of Mexico continental slope. Economic Geology 92, 863–879.

Sassen, R., Losh, S.L., Cathles III., L., Roberts, H.H., Whelan, J.K., Milkov, A.V., et al., 2001. Massive vein-filling gas hydrate: relation to ongoing gas migration from the deep subsurface in the Gulf of Mexico. Marine and Petroleum Geology 18, 551–560.

Shyu, C.T., Hsu, S.K., Liu, C.S., 1998. Heat flows off southwest Taiwan: measurements over mud diapirs and estimated from bottom simulating reflectors. Terrestrial Atmospheric and Oceanic Sciences 9, 795–812.

Sloan, E.D., 1998. Clathrate Hydrates of Natural Gases (Second Edit). Marcel Dekker. Inc., New York p. 628.

Song, H.B., Geng, J.H., Wang, H.K., Zhang, W.S., Fang, Y.X., Hao, T.Y., et al., 2001. A preliminary study of gas hydrates in Dongsha region north of South China Sea. Chinese Journal of Geophysics 44, 687–695 (in Chinese).

Stakes, D.S., Orange, D., Paduan, J.B., Salamy, K.A., Maher, N., 1999. Cold-seeps and authigenic carbonate formation in Monterey Bay, California. Marine Geology 159, 93–109.

Suess, E., Torres, M.E., Bohrmann, G., Collier, R.W., Greinert, J., Linke, P., et al., 1999. Gas hydrate destabilization: enhanced dewatering, benthic material turnover and large methane plumes at the Cascadia convergent margin. Earth and Planetary Science Letters 170, 1–15.

Valentine, D.L., Reeburgh, W.S., 2000. New perspectives on anaerobic methane oxidation. Environmental Microbiology 2, 477–484.

Wray, J.L., 1977. Calcareous Algae. Elsevier Scientific Publishing Company, New York.

Wu, B., Zhang, G., Zhu, Y., Lu, Z., Chen, B., 2003. Progress of gas hydrate investigation in China offshore. Earth Science Frontiers 10, 177–189 (in Chinese).

Wu, S., Zhang, G., Huang, Y., Liang, J., Wong, H.K., 2005. Gas hydrate occurrence on the continental slope of the northern South China Sea. Marine and Petroleum Geology 22, 403–412.

Xue, W.J., Huo, C.L., Si, G.X., Zhu, W.Q., Xia, Z., 1991. Late quaternary palaeoclimatology and palaeooceanography of the central-northern South China Sea. Geological Research of South China Sea 4, 1–96 (in Chinese).